Supplementary Information for Electronic correlations and partial gap in the bilayer nickelate $La_3Ni_2O_7$

Zhe Liu[1,*], Mengwu Huo[2,*], Jie Li[1,*], Qing Li[1], Yuecong Liu[1], Yaomin Dai[1,†], Xiaoxiang Zhou[1], Jiahao Hao[1], Yi Lu[1,†], Meng Wang[2,†], & Hai-Hu Wen[1,†]

[1]*National Laboratory of Solid State Microstructures and Department of Physics, Collaborative Innovation Center of Advanced Microstructures, Nanjing University, Nanjing 210093, China*

[2]*Center for Neutron Science and Technology, Guangdong Provincial Key Laboratory of Magneto-electric Physics and Devices, School of Physics, Sun Yat-Sen University, Guangzhou, Guangdong 510275, China*

[*]These authors contributed equally to this work.

[†]email: ymdai@nju.edu.cn; yilu@nju.edu.cn; wangmeng5@mail.sysu.edu.cn; hhwen@nju.edu.cn

Supplementary Note 1

The band theory electron's kinetic energy is proportional to the square of the calculated plasma frequency $\omega_{p,\text{cal}}$ for the intraband response[1]

$$K_{\text{band}} = \frac{c_0 \omega_{p,\text{cal}}^2}{120\pi ec}, \tag{1}$$

where c_0 is the c-axis lattice parameter which is 20.455 Å for $La_3Ni_2O_7$[2]. In this equation, both K_{band} and $\omega_{p,\text{cal}}$ are in units of eV, and other quantities are in SI units. DFT calculations directly give $\omega_{p,\text{cal}}$ = 3.22 eV for $La_3Ni_2O_7$ (Supplementary Note 2). Hence, we get K_{band} = 1.17 eV.

Similarly, the experimental kinetic energy of electrons can be written as

$$K_{\text{exp}} = \frac{c_0 \omega_{p,\text{exp}}^2}{120\pi ec}, \tag{2}$$

where $\omega_{p,\text{exp}}$ represents the Drude plasma frequency in the experimental $\sigma_1(\omega)$, which can be extracted from a Drude-Lorentz analysis of the measured $\sigma_1(\omega)$.

Based on Eqs. (1) and (2), we find

$$\frac{K_{\text{exp}}}{K_{\text{band}}} = \frac{\omega_{p,\text{exp}}^2}{\omega_{p,\text{cal}}^2}. \tag{3}$$

Supplementary Note 2

The plasma frequency in Wien2k is obtained from the integral of the squared band velocities at the Fermi level:

$$\omega_{p,ii}^2 = \frac{4\pi e^2}{\hbar^2} \sum_n \int \frac{d\mathbf{k}}{V} v_{ii,n}^2(\mathbf{k}) \delta(\epsilon_n(\mathbf{k}) - \epsilon_F), \tag{4}$$

where ii represents xx, yy and zz; n is the band index; v and V correspond to the band velocity and the normalization volume, respectively. This equation (without broadening) directly yields $\omega_{p,xx}$ = 3.2186 eV, $\omega_{p,yy}$ = 3.2206 eV, and $\omega_{p,zz}$ = 0.3918 eV for $La_3Ni_2O_7$. Since the optical spectra were measured in the ab planes and $La_3Ni_2O_7$ crystallizes in the orthorhombic $Amam$ structure, we take $\omega_{p,\text{cal}}^2 = (\omega_{p,xx}^2 + \omega_{p,yy}^2)/2$ and get $\omega_{p,\text{cal}}$ = 3.22 eV and K_{band} = 1.17 eV for $La_3Ni_2O_7$. Different broadening factors (0.01 eV, 0.02 eV, and 0.03 eV) were used, but resulted in the same value for $\omega_{p,\text{cal}}$, suggesting that the broadening factor has no influence on the determination of $\omega_{p,\text{cal}}$. Actually, within Wien2k, the broadening factor is just an arbitrary parameter basically to plot the intraband contribution. What the code calculates is only the plasma frequency, and based on the chosen broadening it just adds an arbitrary Drude contribution. Therefore, we don't expect to see the plasma frequency changes with different broadenings.

The inclusion of Hubbard U (DFT + U), which allows for the incorporation of local Coulomb interactions for the Ni-3d orbitals, may induce small changes of the band structure, thus changing the value of $\omega_{p,\text{cal}}$. However, for a study of the electronic correlation effect in $La_3Ni_2O_7$, it is more reasonable to compare the experimental results to the calculations without including the Hubbard U. Therefore, the Hubbard U was not included in the DFT calculations.

Supplementary Note 3

Oxygen deficiencies may exist in the $La_3Ni_2O_7$ samples, leading to a slight self-doping. Transport studies on $La_3Ni_2O_7$ have shown that 0.07 (1%) oxygen deficiencies can change the resistivity from a metallic to insulating temperature dependence[3,4]. The temperature-dependent resistivity curve of our crystal exhibits metallic behavior down to 2 K, indicating that the content of oxygen deficiencies in our sample is lower than 0.07. Here, we consider an oxygen deficiency content of 0.1, which corresponds to a doping of 0.2 electrons per unit cell. After considering the self-doping effect, the Fermi level is shifted upwards by 13 meV, and the calculated $\sigma_1(\omega)$ is shown in Supplementary Figure 4c. While the interband response changes somewhat comparing to the calculated $\sigma_1(\omega)$ for the stoichiometric $La_3Ni_2O_7$ (Supplementary Figure 4b), no significant change is found for the Drude (intraband) component. The Drude weight is still strikingly larger than that in the measured $\sigma_1(\omega)$ (Supplementary Figure 4a), pointing to strong electronic correlations in $La_3Ni_2O_7$. The plasma frequency from the calculation is $\omega_{p,\mathrm{cal}}$ = 3.25 eV, which gives $K_{\mathrm{exp}}/K_{\mathrm{band}}$ = 0.022.

	Resonance frequency ω_0 (cm^{-1})	Plasma frequency ω_p (cm^{-1})	$1/\tau$ or γ (cm^{-1})
D1	–	3166	178
D2	–	2180	232
L1	813	4449	2072
L2	2866	4602	2389
L3	6628	11910	4741
L4	10476	16974	7902
L5 (LH)	18265	14857	13309
L6 (LH)	28818	17263	15242
L7 (LH)	46944	45697	21495

Supplementary Table 1 | Drude-Lorentz fitting parameters for $\sigma_1(\omega)$ of $La_3Ni_2O_7$ at 150 K. The fitting parameters for the two Drude components and a series of Lorentz components used to fit $\sigma_1(\omega)$ of $La_3Ni_2O_7$ at 150 K. LH represents the sum of three Lorentz components (L5, L6 and L7) in the high-frequency range.

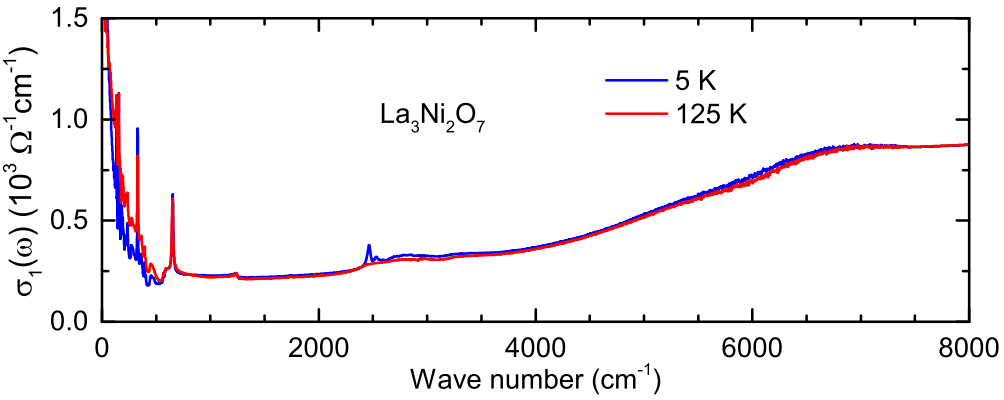

Supplementary Figure 1 | The optical conductivity $\sigma_1(\omega)$ of $La_3Ni_2O_7$. The red and blue curves denote $\sigma_1(\omega)$ of $La_3Ni_2O_7$ up to 8000 cm^{-1} above (125 K) and below (5 K) the transition, respectively. Below the transition, i.e. at 5 K, the low-frequency Drude response is suppressed and the spectral weight is transferred to a broad frequency range (about 600–6500 cm^{-1}).

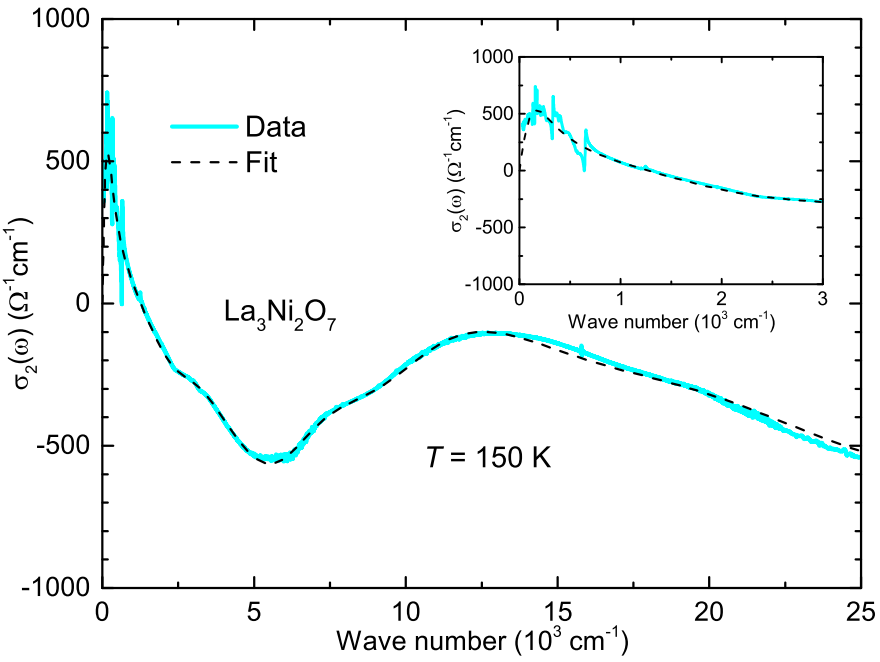

Supplementary Figure 2 | Fitting result for $\sigma_2(\omega)$ of $La_3Ni_2O_7$ at 150 K. The cyan solid curve is the experimental $\sigma_2(\omega)$ of $La_3Ni_2O_7$ at 150 K; the dashed line through the data is the Drude-Lorentz fit using the same parameters as that used for the fit of $\sigma_1(\omega)$. The inset shows the fitting result in the low-frequency range.

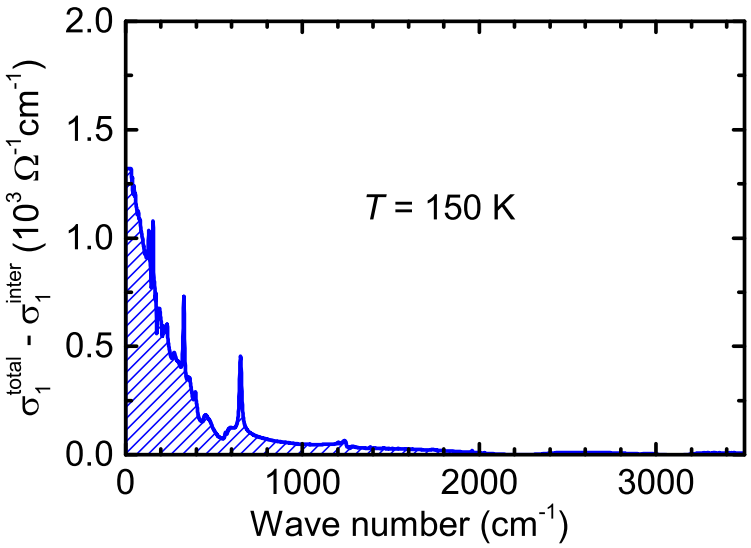

Supplementary Figure 3 | The optical conductivity of $La_3Ni_2O_7$ with interband contributions removed. The optical conductivity after the interband contributions are removed ($\sigma_1^{\text{total}} - \sigma_1^{\text{inter}}$) for $La_3Ni_2O_7$ at 150 K.

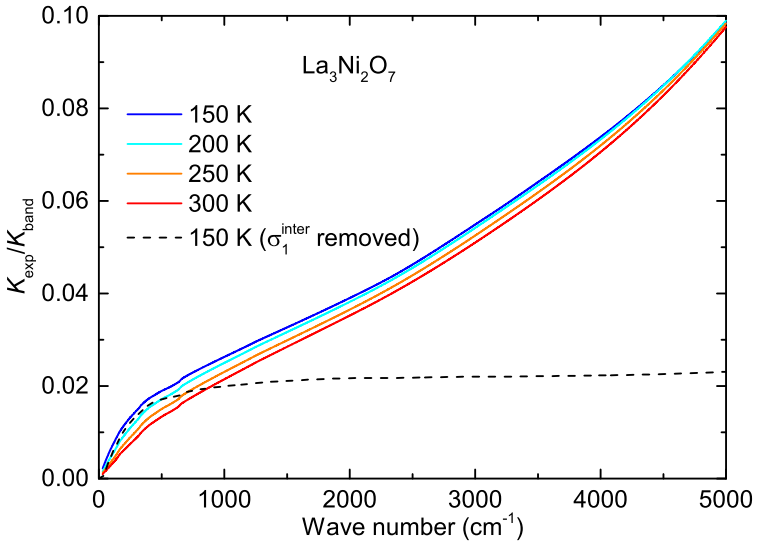

Supplementary Figure 4 | $K_{\mathbf{exp}}/K_{\mathbf{band}}$ **as a function of the cutoff frequency for different temperatures.** The solid curves denote $K_{\rm exp}/K_{\rm band}$ as a function of the cutoff frequency for different temperatures above T^*. Due to the presence of low-energy interband transitions, significant contributions from interband transitions are included, leading to a monotonic increase of $K_{\rm exp}/K_{\rm band}$ with increasing cutoff frequency for all temperatures. If we remove the interband contributions from $\sigma_1(\omega)$, as shown by the dashed line, $K_{\rm exp}/K_{\rm band}$ quickly saturates and converges to the value of $\sim$0.022.

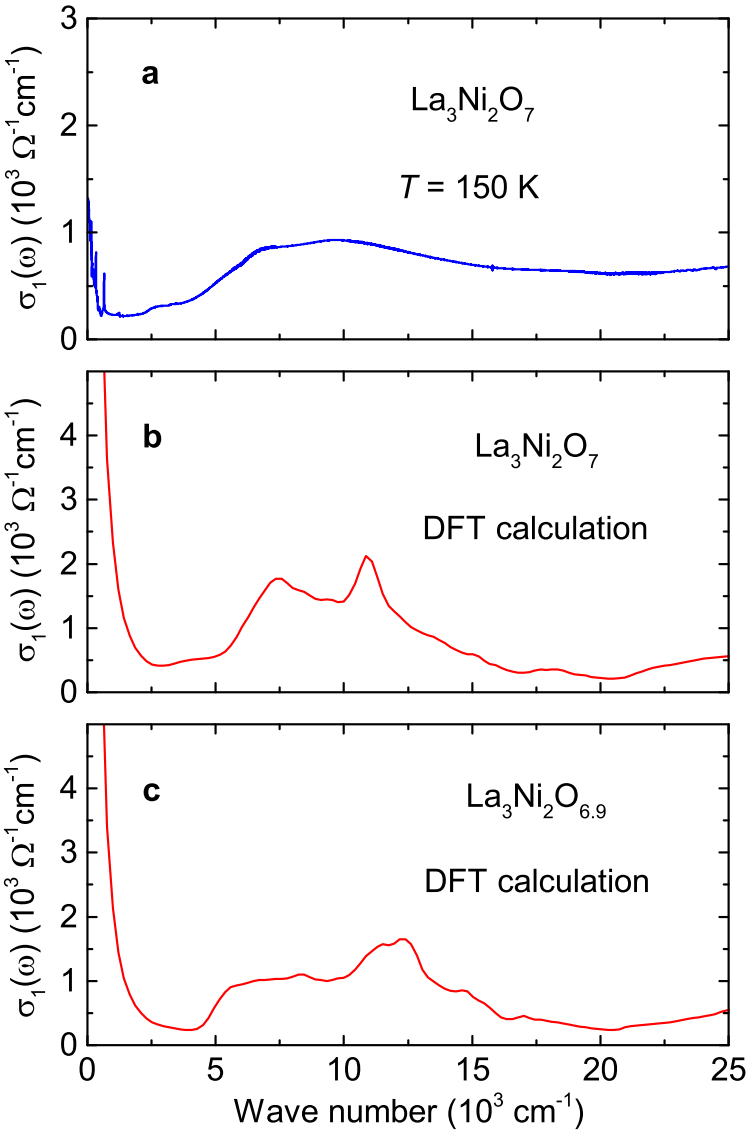

Supplementary Figure 5 | Experimental and calculated optical conductivity. a The measured $\sigma_1(\omega)$ at 150 K for $La_3Ni_2O_7$. **b** The calculated $\sigma_1(\omega)$ for the stoichiometric $La_3Ni_2O_7$. **c** The calculated $\sigma_1(\omega)$ for $La_3Ni_2O_{6.9}$ with slight oxygen deficiencies.

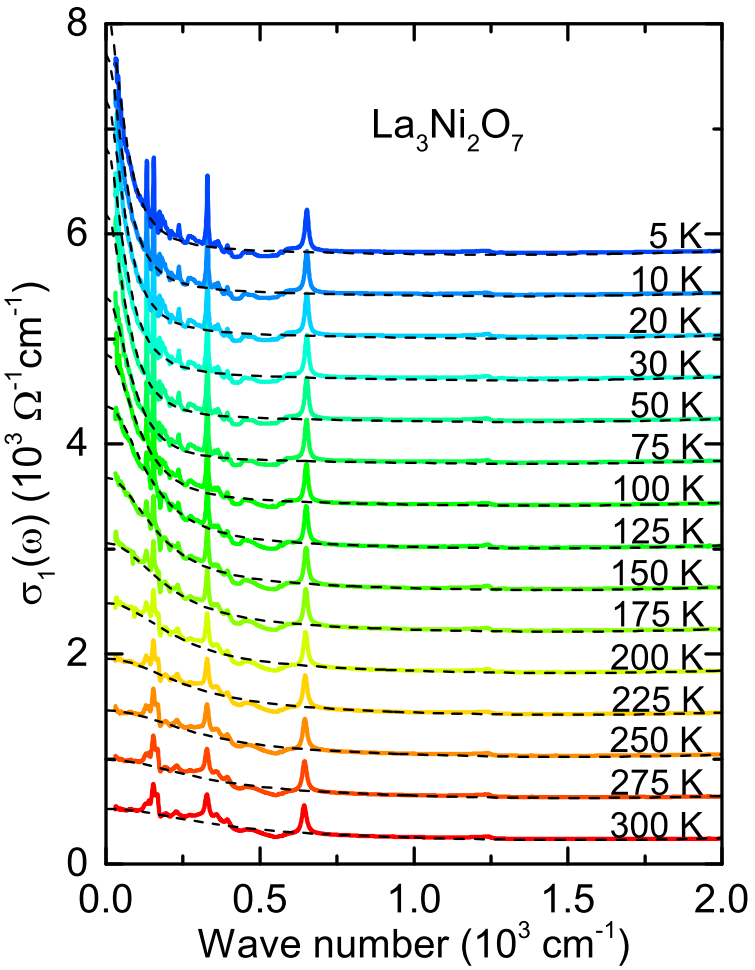

Supplementary Figure 6 | The Drude-Lorentz fit for $\sigma_1(\omega)$ of $La_3Ni_2O_7$ at different temperatures. The solid curves denote the measured $\sigma_1(\omega)$ of $La_3Ni_2O_7$ at different temperatures; the dashed lines through the data represent the Drude-Lorentz fitting results at corresponding temperatures.

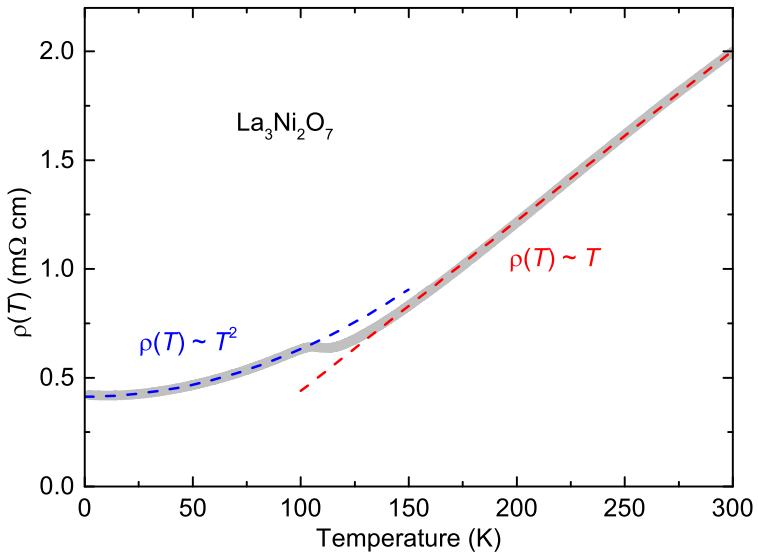

Supplementary Figure 7 | The temperature-dependent resistivity $\rho(T)$ of $La_3Ni_2O_7$. The gray solid curve denotes the measured temperature-dependent resistivity $\rho(T)$ of $La_3Ni_2O_7$. The red dashed line is a linear fit of the high-temperature $\rho(T)$; the blue dashed line is a quadratic temperature dependence fit of $\rho(T)$ below T^*.

References

1. Qazilbash, M. M. *et al.* Electronic correlations in the iron pnictides. *Nat. Phys.* **5**, 647–650 (2009).

2. Liu, Z. *et al.* Evidence for charge and spin density waves in single crystals of $La_3Ni_2O_7$ and $La_3Ni_2O_6$. *Sci. China Phys. Mech. Astron.* **66**, 217411 (2023).

3. Taniguchi, S. *et al.* Transport, Magnetic and Thermal Properties of $La_3Ni_2O_{7-\delta}$. *J. Phys. Soc. Jpn.* **64**, 1644–1650 (1995).

4. Wang, G. *et al.* Pressure-Induced Superconductivity In Polycrystalline $\mathrm{La_3Ni_2O_{7-\delta}}$. *Phys. Rev. X* **14**, 011040 (2024).